IRON AND MOLYBDENUM DIFFUSION IN $Fe_{76}Mo_8B_{15}Cu_1$ ALLOY

JIŘÍ ČERMÁK*, IVO STLOUKAL

Institute of Physics of Materials, AS CR, Žižkova 22, CZ-61662 Brno, Czech Republic

Received 10 August 2005, accepted 13 September 2005

Fe and Mo tracer diffusion in $Fe_{76}Mo_8B_{15}Cu_1$ alloy was studied using serial sectioning method in the temperature range 527–649 K. The ribbon-like samples were annealed at 695 K for 1 and 5 hours before the diffusion experiments; the volume fraction of crystalline phase was checked by the Mössbauer spectroscopy. Concentration profiles obtained by sputtering by Ar^+ ions in a glow discharge show two distinct branches suggesting that two diffusion paths are operating. Arrhenius plot of measured diffusion coefficients was not linear in the whole temperature studied interval, which may be due to predominance of less energetically demanding jumps at lower temperatures and higher effective activation enthalpy at higher temperatures. The kink temperature was about 630 K.

K e y w o r d s: amorphous materials, nanocrystalline materials, diffusion

1. Introduction

Amorphous alloys serve as precursors for nanocrystalline materials, which represent a very interesting group of functional materials with high potential for industry. They show, e.g., excellent magnetic parameters caused by presence of fine nanograins in the amorphous matrix [1]. The most frequent types of nanostructured magnetic materials are known as FINEMET [2] or NANOPERM [3]. Since they are applied in thermodynamically unstable state, the knowledge of their diffusion properties both in amorphous and in nanostructured state are very important for the production technology.

The formation of nanocrystalline grains in disordered matrix is a complex process involving the nucleation of crystallites and their growth – both being influenced by optimized chemical composition of respective alloy. Since the crystallites in NANOPERM–type alloys are formed by the α-Fe grains, the Mössbauer spectroscopy is often applied to the monitoring the crystallization process in these alloys [4, 5].

*corresponding author, e-mail: cermak@ipm.cz

Diffusion measurement in amorphous state is affected by the fact that the alloys are not in the thermodynamically stable state. As a rule, the diffusion coefficient measured in an isothermal experiment decreases with time due to the relaxation of free volume in the amorphous structure. The more or less stationary values of diffusion coefficients can be achieved first after a certain relaxation time needed to stabilize the structure [6, 7]; this relaxation precedes the crystallization itself.

As for diffusion mechanism in amorphous alloys, two cases are commonly distinguished (see, e.g., in [8]): (i) direct diffusion mechanism, which is not mediated by any defect (diffusion of small atoms) and (ii) indirect mechanism mediated by quasi-vacancies. Any case, in the amorphous alloys, the diffusion jump involves, in a more or less extent, the motion of neighboring atoms (collective motion – applies especially by diffusion of large atoms).

This paper reports on iron and molybdenum tracer diffusion measurements in annealed $Fe_{76}Mo_8B_{15}Cu_1$ alloy, which belongs to NANOPERM-type materials. Iron and molybdenum are elements that are responsible for the desired structure and functional characteristics of the alloy and, hence, the knowledge of their diffusion characteristics can contribute to better understanding of processes controlled by mobility of alloy components.

2. Experimental

2.1 Sample preparation

The experimental amorphous alloy was prepared by the single roller melt-spinning technique in argon atmosphere at Department of Nuclear Physics and Technology, Slovak University of Technology Bratislava, Slovak Republic. Ribbons of $Fe_{76}Mo_8B_{15}Cu_1$ were about 6 mm wide and 20 μm thick. The diffusion samples were cut from the ribbons and their shiny (air) side was metalographically ground using SiC papers and finally polished with diamond paste. Total thickness removed from the surface was about 2 μm.

The samples were wrapped into Ta foil and sealed in evacuated silica ampoules (residual pressure less than 3×10^{-4} Pa). To relax the structure of samples, they were annealed at 695 K for 1 and 5 hours, respectively. The fraction of crystalline phase after the relaxation did not exceed the sensitivity threshold of Mössbauer measurement.

2.2 Radiotracer measurements

The radiotracer ^{59}Fe was used in a form of aqueous solution of iron chloride, and the radiotracer ^{99}Mo as an aqueous solution of ammonium molybdate. The thin layer of radioisotope was deposited on the polished surface using two methods: (i) vacuum evaporation technique (Fe tracer), and (ii) direct dripping of the radioisotope on the sample surface (both Fe and Mo tracers). In the first case, a

drop of the radioisotope on tungsten boat was dried in air by infrared lamp and decomposed in vacuum into iron and chlorine. After that, the iron was evaporated by a thermal shock on the sample surfaces mounted in a cold holder. The thickness of the radioactive layer was in order of 10^{-9} m.

Since a considerable crystallization (about 30 % of crystalline phase) was caused by the thermal shock used for the deposition of the radioactive layer by the vacuum evaporation technique, the radioactive layer was alternatively deposited by dripping-and-drying technique. The small amount (about 8×10^{-3} cm^3) of the water solution with radioisotope was dropped direct on the annealed (695 K/1 h) sample surface and subsequently it was dried by infrared lamp.

The diffusion measurements were carried out in the horizontal tube furnace in the temperature range 527–649 K. The samples were encapsulated in the Ta envelope and sealed in evacuated silica ampoules. The annealing temperature was checked by a Pt-PtRh thermocouple and stabilized within ± 1 K.

The amount of crystallized phase was checked by Mössbauer measurement after the diffusion anneals. The amount of crystalline phase in vacuum-deposited samples remains unchanged (about 30 % – independent on the duration of relaxation pre-annealing), in samples with dripped-and-dried radioactive layers the fraction of crystalline phase was up to some 5 %.

The penetration profiles were obtained by serial sectioning method. The individual layers were removed using DC-glow discharge sputtering with Ar^+ ions [9]. The apparatus consists of two electrodes in a vacuum recipient; one of them holds the sample, the second one is carrousel with Al foils. During sputtering process, the removed material is collected on aluminum foils that are changed in the chosen time interval. The sputtering conditions are defined by voltage between the electrodes and by Ar pressure.

After sputtering, the individual Al foils are separately placed in plastic vials, dissolved in a small amount (0.7 cm^3) of a dilute HCl (water : HCl = 1 : 1) and mixed with scintillation cocktail. After that, they are counted in a Liquid Scintillation Counter TRI-CARB 3170 TR/LS. The measured relative activity of the vial is proportional to the average concentration of diffusant in respective layer.

The penetration depth x is proportional to sputter time and sputter rate, which is measured at the same sample and for the same sputtering conditions after a long time-sputtering (a couple of hours) at the conclusion of each sputter run. The total mass deficit of the sample is measured by precise weighting.

3. Concentration profiles

The typical penetration profile obtained by DC-glow discharge sputtering is shown in Fig. 1. It can be seen that the profile is composed of four segments: The first one (I.) is limited to very narrow area by the surface. Here the measured radioactivity increases with increasing depth co-ordinate x. This segment is due to

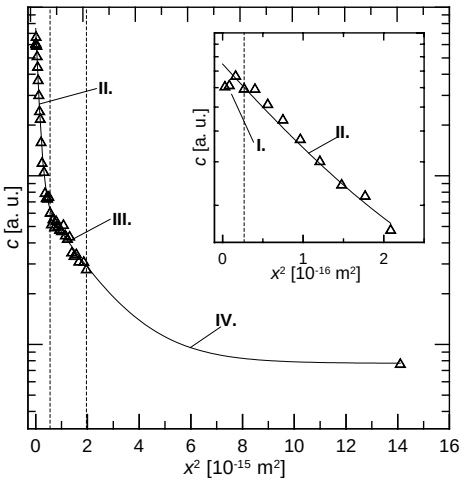

Fig. 1. An example of penetration profile $c(x,t)$ with characteristic segments (I.–IV.). Full line – Eq. (1), small picture – detail of the beginning of the profile.

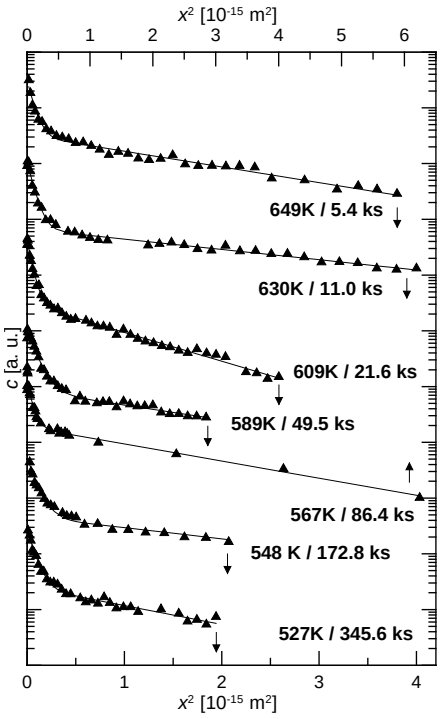

Fig. 2. Penetration profiles $c(x,t)$ for ^{59}Fe self-diffusion in experimental alloy annealed at 695 K for 1 hour (vacuum evaporated).

cascade-mixing effect [10, 11] by the surface. At greater depths x, there is a steeply decreasing second segment (II.) followed by the third one (III.), which slope is expressively lower than that of the second segment. The fourth segment (IV.) is a tail that reveals the background. It is represented by the last point in Fig. 1 that was measured at each curve in order to obtain a well-defined sputter rate and a value that was used for background correction. Since it was found that both the second and the third segments were linear in coordinates $\log c$ vs. x^2, we suggest an existence of two different diffusion paths that correspond to two amorphous phases in experimental materials. The presence of such phases was observed in similar materials by Walter *et al.* [12] or by Miglierini *et al.* [13]. Hence, the experimental penetration curve was fitted by equation

$$c'(x,t) = A\exp\left(-\frac{x^2}{4D_1 t}\right) + B\exp\left(-\frac{x^2}{4D_2 t}\right) + C, \qquad (1)$$

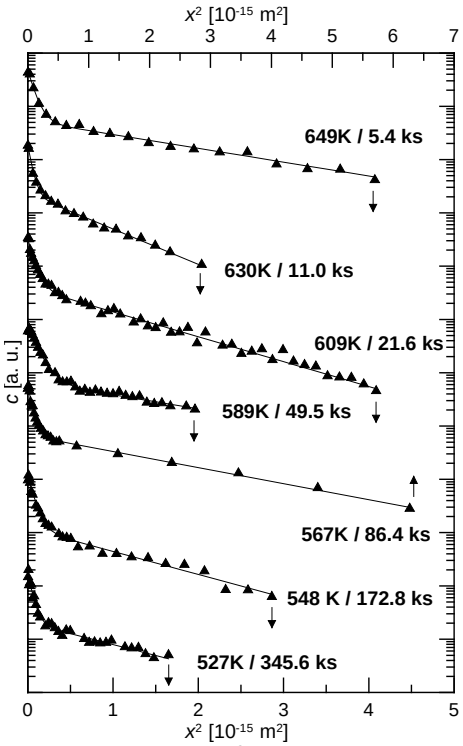

Fig. 3. Penetration profiles $c(x,t)$ for ^{59}Fe self-diffusion in experimental alloy annealed at 695 K for 5 hours (vacuum evaporated).

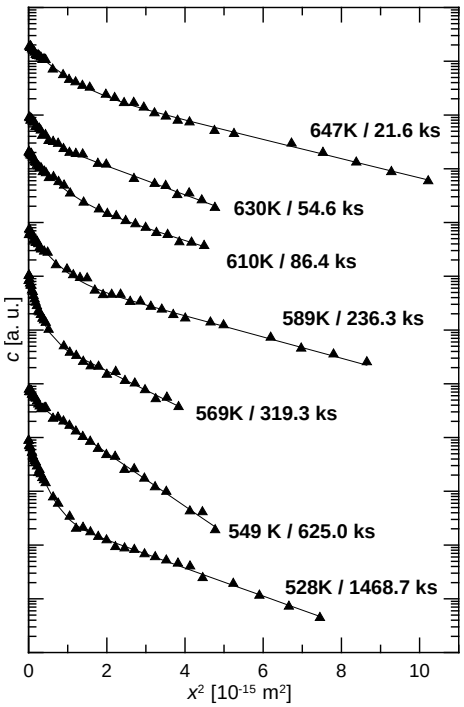

Fig. 4. Penetration profiles $c(x,t)$ for ^{59}Fe self-diffusion in experimental alloy annealed at 695 K for 1 hour (dripped and dried).

where coefficients A, D_1, D_2 and C (D_1 and D_2 – diffusion coefficients, C – background) were obtained as fitting parameters; the fit quality is demonstrated by the full line in Fig. 1. The background-corrected penetration profiles, i.e. $\log c(x,t)$ vs. x^2 ($c = c' - C$) are shown in Figs. 2–5.

4. Results and discussion

4.1 Diffusion of ^{59}Fe

The iron tracer diffusion measurements were carried out in the temperature interval 527–649 K. Measured curves $c'(x,t)$ were fitted by Eq. (1) and obtained diffusion coefficients D_1 and D_2 are summarized in Tables 1–3.

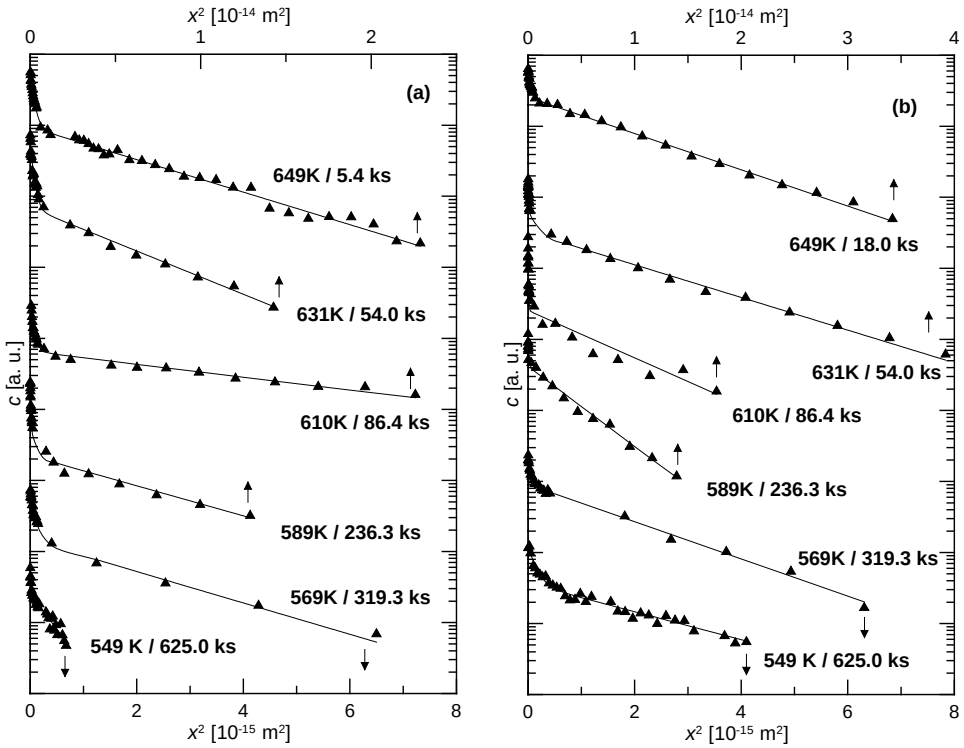

Fig. 5. Penetration profiles $c(x,t)$ for ^{99}Mo diffusion in experimental alloy annealed at 695 K for 1 hour (dripped and dried) for 1$^{\text{st}}$ (a) and 2$^{\text{nd}}$ (b) set of measurements.

Table 1. The parameters of ^{59}Fe self-diffusion in $Fe_{76}Mo_8B_{15}Cu_1$ alloy annealed at 695 K for 1 hour (vacuum evaporated). T and t are the temperature and time of diffusion anneal, D_1 and D_2 are obtained diffusion coefficients

T [K]	t [s]	1 hour		5 hours	
		D_1 [m$^2\cdot$s^{-1}]	D_2 [m$^2\cdot$s^{-1}]	D_1 [m$^2\cdot$s^{-1}]	D_2 [m$^2\cdot$s^{-1}]
649	5400	2.94×10^{-21}	8.29×10^{-20}	3.32×10^{-21}	7.75×10^{-20}
630	11040	9.85×10^{-22}	2.55×10^{-20}	1.02×10^{-21}	1.48×10^{-20}
609	21600	5.49×10^{-22}	9.73×10^{-21}	7.92×10^{-22}	1.08×10^{-20}
589	49500	4.42×10^{-22}	8.38×10^{-21}	5.51×10^{-22}	8.29×10^{-21}
567	86400	1.96×10^{-22}	6.34×10^{-21}	2.06×10^{-22}	5.84×10^{-21}
548	172800	6.88×10^{-23}	1.52×10^{-21}	1.00×10^{-22}	1.46×10^{-21}
527	345600	3.97×10^{-23}	8.41×10^{-22}	3.70×10^{-23}	7.64×10^{-22}

Table 2. The parameters of ^{59}Fe self-diffusion in $Fe_{76}Mo_8B_{15}Cu_1$ alloy annealed at 695 K for 1 hour (dripped and dried). T and t are the temperature and time of diffusion anneal, D_1 and D_2 are obtained diffusion coefficients

T [K]	t [s]	D_1 [m^2·s^{-1}]	D_2 [m^2·s^{-1}]
647	21600	6.26×10^{-21}	2.81×10^{-20}
630	54600	1.21×10^{-21}	7.43×10^{-21}
610	86400	1.23×10^{-21}	5.44×10^{-21}
589	236340	4.14×10^{-22}	2.33×10^{-21}
569	319260	1.25×10^{-22}	9.48×10^{-22}
549	624981	5.80×10^{-23}	3.50×10^{-22}
528	1468680	3.92×10^{-23}	2.83×10^{-22}

Table 3. The parameters of ^{99}Mo self-diffusion in $Fe_{76}Mo_8B_{15}Cu_1$ alloy annealed at 695 K for 1 hour (dripped and dried). T and t are the temperature and time of diffusion anneal, D_1 and D_2 are obtained diffusion coefficients

T [K]	t [s]	D_1 [m^2·s^{-1}]	D_2 [m^2·s^{-1}]
649	5400	9.52×10^{-21}	2.75×10^{-19}
649	18000	3.26×10^{-21}	1.18×10^{-19}
631	54000	8.07×10^{-22} 4.51×10^{-22}	2.07×10^{-20} 4.37×10^{-20}
610	86400	4.67×10^{-22} 1.01×10^{-22}	4.15×10^{-20} 1.89×10^{-20}
589	236340	6.45×10^{-23} 1.58×10^{-23}	6.79×10^{-21} 4.04×10^{-21}
569	319260	6.36×10^{-23} 3.70×10^{-23}	1.54×10^{-21} 1.30×10^{-21}
549	624981	4.94×10^{-24} 5.36×10^{-23}	1.75×10^{-22} 8.82×10^{-22}

The temperature dependence of D's is shown in Fig. 6 in comparison with the literature data on iron self-diffusion in amorphous $Fe_{80}B_{20}$ [14], $Fe_{40}Ni_{40}B_{20}$ [15], and $Fe_{68}Co_{17}B_{15}$ [16].

It can be seen that no significant difference in D_1 between specimens with drip-and-dried (annealed for 1 h at 695 K) and evaporation deposited radioactive layer (that were annealed for 1 h and 5 h at 695 K) was observed. Therefore, it may be concluded that the values of D_1 characterize the diffusion in the residual amorphous phase.

On the other hand, values of D_2 measured in samples with smaller volume fraction of crystallized phase are significantly lower than those obtained for samples with higher amount of crystalline phase. Therefore, it seems that the deeper part

of the concentration profiles (giving the D_2) can be related to the presence of crystalline phase (or: to the presence of interface between crystallites and rest matrix) [13].

Comparing the present results with literature data reported for Fe diffusion in similar materials one can see that whereas at highest temperatures 630––649 K, the present D's agree reasonably with the literature, at lower temperatures the present data show an up-ward curvature. It is known that the diffusion in an amorphous alloy is realized by jumps with varied activation enthalpies. If only the mechanism of diffusion is the same at all diffusion temperatures, the effective value preserves and the temperature dependence of diffusion coefficient is Arrhenius-like. The temperature dependence of D's observed in the present paper may be caused by the fact that whereas at higher temperatures jumps with higher activation prevail, at lower temperature the diffusion of Fe occurs prevailingly via jumps with lower activation enthalpy.

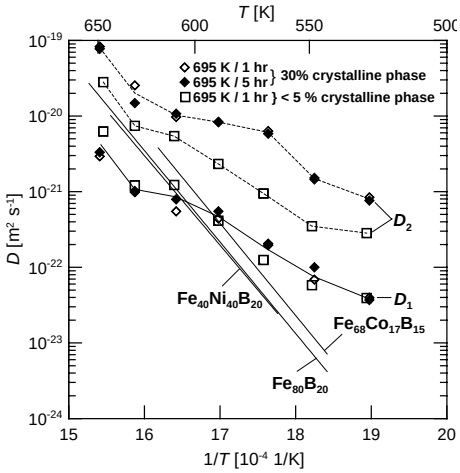

Fig. 6. Temperature dependence of D for Fe self-diffusion in experimental alloy (open diamonds – tracer evaporated, full diamonds and open squares – tracer dripped and dried) compared with data on Fe self-diffusion in amorphous $Fe_{80}B_{20}$ [14], $Fe_{40}Ni_{40}B_{20}$ [15], and $Fe_{68}Co_{17}B_{15}$ [16].

4.2 Diffusion of ^{99}Mo

The molybdenum tracer diffusion has been measured in the temperature interval 549–649 K. Similar to Fe diffusion, two diffusion coefficients were evaluated from experimental curves. The obtained penetration profiles in coordinates $\log c$ vs. x^2 are shown in Fig. 5. The diffusion coefficients D_1 and D_2 listed in Table 3 have been calculated by the same mathematical procedure as in the case of iron self-diffusion. They are plotted against temperature in Fig. 7 together with data obtained for Fe diffusion.

Observed relations between diffusion coefficients D_i^{X} ($i = 1$ for residual amorphous phase and $i = 2$ for interfacial amorphous phase, X = ^{99}Mo, ^{59}Fe) may be, at least qualitatively, explained by two factors: (i) The greater Mo atoms diffuse slower than Fe atoms, therefore relation $D_1^{\mathrm{Fe}} > D_1^{\mathrm{Mo}}$ was observed. (ii) It may be speculated that Mo atoms are expelled from the growing crystallites and that Mo concentration in interfacial phase is greater than that in the residual amorphous phase. Hence, it may be expected that the mean interatomic distance

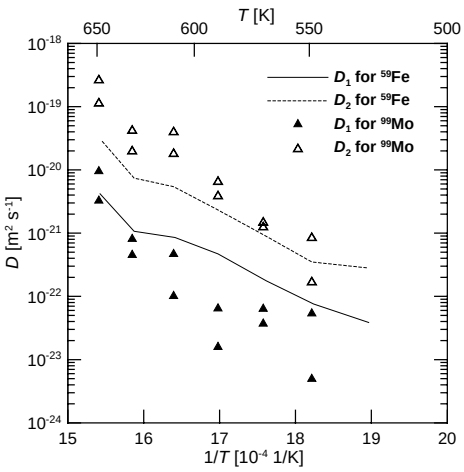

Fig. 7. Temperature dependence of D for Mo self-diffusion (triangles) compared with data on Fe self-diffusion (lines) in amorphous $Fe_{76}Mo_8B_{15}Cu_1$ alloy (all for dripped and dry technique).

in the interfacial amorphous phase is greater than the mean interatomic distance in residual amorphous phase which may explain the observed inequality $D_2^{\mathrm{X}} > D_1^{\mathrm{X}}$. The reversed relation $D_2^{\mathrm{Fe}} < D_2^{\mathrm{Mo}}$ observed for diffusion in interfacial amorphous phase may be explained by a predominance of the second factor in case of Mo (Mo diffusivity is more increased in interfacial phase than that of Fe in the same phase).

5. Summary

In the present work, the Fe and Mo diffusion in annealed $Fe_{76}Mo_8B_{15}Cu_1$ alloy was measured using serial sectioning method in the temperature range 527–649 K. The results can be summarized in following items:

– There are two diffusion paths controlling both Fe and Mo diffusion studied in relaxed amorphous $Fe_{76}Mo_8B_{15}Cu_1$ alloy. The first path is slower and is attributed to residual amorphous phase; the second one is faster and is attributed to interfacial amorphous phase.

– The rate of Fe and Mo diffusion in residual amorphous phase at higher temperatures (630–649 K) is about the same.

– Temperature dependence of diffusion coefficients is curved up-ward. At the highest diffusion temperatures, the Fe diffusion coefficients are close to literature values for Fe diffusion in $Fe_{80}B_{20}$ [14], in $Fe_{40}Ni_{40}B_{20}$ [15], and in $Fe_{68}Co_{17}B_{15}$ [16]. The curvature of the dependence may be caused by variation in average activation enthalpy of diffusion in amorphous alloy at higher temperatures (atomic jumps with higher activation enthalpy are realized) and at lower temperatures (the jumps with lower activation enthalpy prevail).

Acknowledgements

This work was supported by the Grant Agency of the Czech Republic, contract number 106/04/0228, and by projects of AS CR No. S2041105 and AV0Z20410507. Authors would like to express their thanks to Dr. Y. Jirásková for the Mössbauer measurements.

REFERENCES

[1] HERNANDO, A.: J. Phys.-Condens. Mat., *11*, 1999, p. 9455.
[2] YOSHIZAWA, Y.—OGUMA, S.—YAMAUCHI, K.: J. Appl. Phys., *64*, 1998, p. 6044.
[3] SUZUKI, K.—KATAOKA, N.—INOUE, A.—MAKINO, A.—MASUMOTO, T.: Mater. Trans. JIM, *31*, 1990, p. 743.
[4] MIGLIERINI, M.—GRENECHE, J.-M.—IDZIKOWSKI, B.: Mat. Sci. Eng. A, *304*, 2001, p. 937.
[5] MIGLIERINI, M.—SEBERÍNI, M.—TÓTH, I.—VITÁZEK, K.: J. Magn. Magn. Mater., *265*, 2003, p. 243.
[6] BEKE, D. L.: Key Eng. Mat., *103*, 1995, p. 51.
[7] CLAVAGUERA-MORA, M. T.—CLAVAGUERA, N.—CRESPO, D.—PRADELL, T.: Prog. Mater. Sci., *47*, 2002, p. 559.
[8] FRANK, W.—HORVÁTH, J.—KRONMÜLLER, H.: Mat. Sci. Eng., *97*, 1988, p. 415.
[9] ČERMÁK, J.—STLOUKAL, I.: Phys. Stat. Sol. (a), *158*, 1999, p. 397.
[10] HOFMANN, S.: Surf. Interface Anal., *2*, 1980, p. 148.
[11] HOFMANN, S.: Rep. Prog. Phys., *61*, 1998, p. 827.
[12] WALTER, J. L.—BARTRAM, S. F.—MELLA, I.: Mat. Sci. Eng., *2*, 1978, p. 193.
[13] MIGLIERINI, M.—GRENECHE, J.-M.: J. Phys.-Condens. Matter, *15*, 2003, p. 5637.
[14] HORVÁTH, J.—OTT, J.—PFAHLER, K.—ULFERT, W.: Mat. Sci. Eng., *97*, 1988, p. 409.
[15] HORVÁTH, J.—MEHRER, H.: Cryst. Latt. Def. and Amorph. Mat., *13*, 1986, p. 1.
[16] PAVLOVSKÝ, J.: Kovove Mater., *32*, 1994, p. 126.